Structural and Optical Properties of ZnO Nanowires Doped with Magnesium

H. Zhuang*, J. Wang, H. Liu, J. Li and P. Xu
Institutions of Semiconductors, Shandong Normal University, Jinan 250014, P.R. China

(Received June 13, 2010; revised version October 25, 2010; in final form December 9, 2010)

ZnO nanowires doped with Mg have been successfully prepared on Au-coated Si (111) substrates using chemical vapor deposition method with a mixture of ZnO, Mg, and activated carbon powders as reactants at 850 ℃. The structural, compositional, morphological and optical properties of the samples were characterized by X-ray diffraction, scanning electron microscopy, transmission electron microscopy, high-resolution transmission electron microscopy, and photoluminescence spectroscopy. The nanowires are single crystalline in nature and preferentially grow up along [0001] direction with the average diameter and length of about 60 nm and several hundred micrometers, respectively, thinner and longer than the results of literature using the similar method. Room temperature photoluminescence spectroscopy shows a blueshift from the bulk band gap emission, which can be attributed to Mg doping that were detected by energy dispersive X-ray analysis EDX in the nanowires. Finally, the possible growth mechanism of crystalline ZnO nanowires is discussed briefly.

PACS: 61.46.Km, 61.72.uj, 81.15.Gh, 78.67.−n

1. Introduction

Semiconductor nanostructures have been considered as promising components for future electronics, photonics, biosensing and nanodevices [1]. At room temperature, with a wide band gap of 3.37 eV and large exciton binding energy of 60 meV, ZnO has been recognized as one of the most important semiconductor materials in scientific research and technological applications [2]. To date, various ZnO nanostructures have been successfully synthesized, including nanorods, nanotubes, nanowires, nanobelt, and nanobridge [3]. A key requirement for many applications involving ZnO is its doping with special elements in order to improve its electrical and optical properties [4], and the doping effect has attracted extraordinary attention.

Recently, various doped ZnO nanostructures with different elements (e.g., Al, Ga, In, Sn, Co and Sb) have been achieved [5–11]. Alloying ZnO with Mg was shown to realize the control of the band gap for the realization of light-emitting devices operating in a wider wavelength region [12] without affecting lattice constant, because ionic radius of Mg (0.57 Å) and Zn (0.60 Å) are almost similar [13], the Zn positions can be easily substituted by Mg under certain conditions.

By far, Mg-doped ZnO nanostructures have been successfully fabricated by a lot of methods, such as nanowires, nanowire arrays and ZnO/MgZnO quantum wells by pulsed laser deposition (PLD) [14–16], nanopillars and nanorods by metal-organic chemical vapor deposition (MOCVD) [17, 18], nanorods, nanowires, ternary nanowires, nanoterapods, nanopagodas and dendritic $Zn_{1-x}Mg_xO$ nanostructures by thermal evaporation [14, 19–23], nanowires by thermal diffusion [24]. Nevertheless, there are only a few reports on Mg-doped ZnO nanowires using a mixture of ZnO and activated carbon powders as source materials reported yet except for Wei et al. [25]. Carbothermal reduction, as a simple and effective method, has been utilized widely. The major advantage of this method should lie in its ability to decrease the temperature from 1975 K (which is essential for ZnO powder to melt) to lower than 1000 K: more specifically, its advantage is in its potential for industrial production. This method can possibly be extended to preparation of many other semiconductor nanowires, such as In_2O_3 [26], SiC [27], SiO_2 [28], Si_3N_4 [29], etc.

In this paper, we reported that high-quality Mg-doped ZnO nanowires were synthesized on Si (111) substrate by CVD method with a mixture of ZnO, Mg, and activated carbon powders as reactants on Au-coated Si (111) substrates at the temperature of 850 ℃ under Ar atmosphere. This growth method allows a continuous synthesis and the process is simple and inexpensive, suitable for commercial scale production. The morphology, crystallinity and optical properties of Mg doped ZnO nanowires were carefully investigated. The average length of the nanowires in our experiment is up to

* corresponding author; e-mail: zhuanghuizhao@sdnu.edu.cn

several hundreds of micrometers, which is much longer than result given by Ref. [25], and the average diameter is smaller. Finally, the growth mechanism is briefly discussed.

2. Experimental details

In our experiment, the preparation process of Mg-doped ZnO nanowires could be fallen into two steps in the whole process.

The first step was that a thin layer of Au films was deposited on Si substrates by sputtering Au target in JCK-500A RF magnetron sputtering system. Si (111) substrates were cleaned by sonicating in toluene, acetone, ethanol, and deionized water for 30 min in sequence. The conditions of sputtering process were as follows: the distance between the substrates and the target was 80 mm; the background pressure was 7×10^{-4} Pa; the working gas was pure Ar ($\geq$ 99.99%) and the working pressure was 2 Pa; the output voltage and output current of the radio frequency generator were 320 V and 50 mA, respectively; the Au sputtering time was 2 s and the thickness of resulting Au thin film was equal to about 12 nm.

The second step was that the Mg-doped ZnO nanowires were synthesized by a chemical vapor deposition (CVD) process, which was done in a conventional horizontal tube furnace (L4513II-2/QWZ). A mixture of ZnO (purity 99.9%), Mg (purity 99.99%) and graphite powders with the mass ratio of 7:2:0.1 was used as the source materials. Both the source materials and the Au-coated Si substrates were placed at a quartz boat with a distance of 2 cm between them. After heating the furnace to 850 ℃ at a rate of 50–100 ℃/min, the flowing Ar (99.999%) gas was introduced into the tube to flush out the residual air at a flow rate of 500 sccm for 5 min. Then the quartz boat loaded with the Si substrates and source materials was quickly inserted into it. The source materials were positioned at the centre of the furnace, and the Si substrates were located downstream of the gas flow to collect products. The temperature was held for 10 min under a constant Ar flow of 150 sccm. Finally, the boat was pulled out and cooled to room temperature under atmosphere, and white cotton-like products appeared on the substrates. In addition, under the same condition except the lack of Mg in the source materials, we have prepared pure ZnO nanowires and have used them for the comparison when taking PL spectra.

The morphology and surface microstructure of the samples were characterized by a Hitachi S-570 scanning electron microscopy (SEM), a Hitachi H-800 transmission electron microscopy (TEM) and a Philips Tecnai-20 high resolution transmission electron microscope (HRTEM). The microstructure and chemical composition of the samples were investigated by a Rigaku D/max-rB X-ray diffraction (XRD) meter with a Cu K_α line and an energy dispersive X-ray energy spectroscopy (EDX) system. The room temperature photoluminescence (PL) spectrum of the products was measured by a FLS920 fluorescence spectrophotometer with a He–Cd laser as the excitation light source at 325 nm.

3. Results and disscussion

3.1. Microstructure analysis

Figure 1 shows the typical XRD pattern of the samples. As seen from Fig. 1, all the diffraction peaks in the pattern can be easily assigned to hexagonal wurtzite ZnO, which are in agreement with the reported standard values (JCPDS No. 36-1451). The (002) diffraction peak at $2\theta = 34.58°$ has a slight shift from the standard for bulk ZnO (34.40°) [30], indicating that Mg^{2+} has incorporated into the ZnO host lattice and substitutes for Zn^{2+}, as the ionic radius of Mg^{2+} (0.057 nm) is smaller than Zn^{2+} (with an ionic radius 0.060 nm). No diffraction peaks from metallic Zn and Mg or other phase have been found, revealing that Mg doping has not changed the wurtzite structure of ZnO because of its small content, which is also compatible with results from the substitution of Mg for Zn site and previous reports [22]. In addition, the sharp diffraction peaks reveal that the ZnO nanowires possess good crystalline quality. Au diffraction peaks are not detected by XRD, due to the small size of Au particles (about 3 nm).

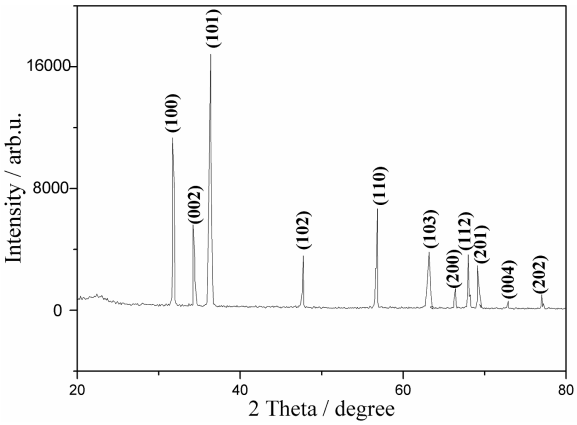

Fig. 1. XRD pattern of Mg-doped ZnO nanowires with a hexagonal wurtzite structure.

3.2. Surface morphology

Surface morphology of the samples and nanowires dimensions were determined by SEM. Figure 2 shows the typical SEM images of the as-synthesized samples at different magnifications. Figure 2a depicts that the morphology of the nanostructures consists of high-density ZnO nanowires. These nanowires interwine with each other and distribute on the whole substrate surface randomly. A magnified SEM image (Fig. 2b) shows that the typical diameter and length are about 60 nm and several hundred micrometers, respectively. In addition, no metal particle is observed at the tops of the nanowires.

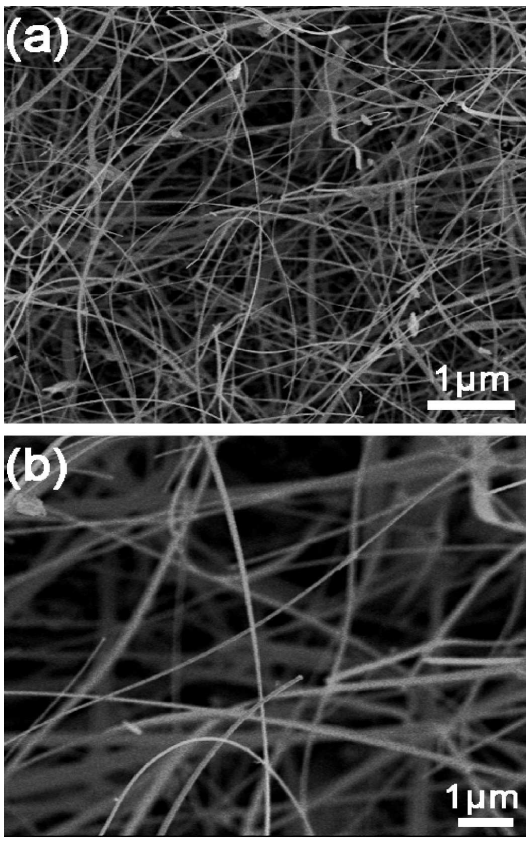

Fig. 2. Typical SEM images of the Mg-doped ZnO nanowires at different magnifications.

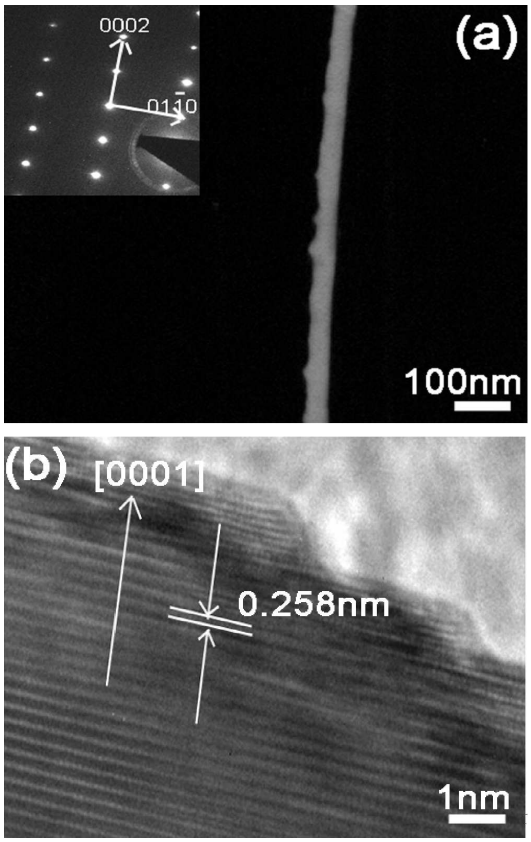

Fig. 3. (a) TEM image of single Mg-doped ZnO nanowire and the correspoding SAED pattern, (b) HRTEM image of the nanowire.

For better understanding of the morphology properties, TEM, HRTEM and selected area electron diffraction (SAED) pattern were employed to further investigate the as-synthesized ZnO nanostructures, as shown in Fig. 3a,b.

As shown in Fig. 3a, TEM image of a single ZnO nanowire reveals that the ZnO nanowire has a diameter of about 60 nm, and its surface is coarse, which may be attributed to the defects from Mg doping during growth. The inset of Fig. 3a shows the selected area electron diffraction (SAED) pattern of the Mg-doped ZnO nanowires, which demonstrates that the nanowires have a high crystal quality due to the regular electron diffraction pattern. The SAED pattern is consistent with the hexagonal wurtzite structure of ZnO with no second phase detected. Therefore, we can conclude that the Mg doping did not perturb significantly the lattice structure of the ZnO matrix.

Figure 3b shows the HRTEM lattice image of the single Mg-doped ZnO nanowire, the visible lattice fringes disclose that the nanowire is high quality hexagonal wurtzite single crystalline grown along [0001] direction. The lattice spacing between the two (0002) fringes is 0.258 nm, which is slightly smaller than the plane distance (0.260 nm) of undoped ZnO (0002). This finding can be explained as the result of a random distribution of Mg ions replacing Zn in the ZnO crystal lattice. This confirms that introduction of divalent Mg^{2+} in the ZnO lattice did not affect the growth direction.

3.3. Chemical composition analysis

Corresponding chemical composition of the synthesized ZnO nanowires were determined by EDX spectroscopy. Figure 4 shows a typical EDX spectrum of the edge of the nanowires. It is clear that only the Zn,

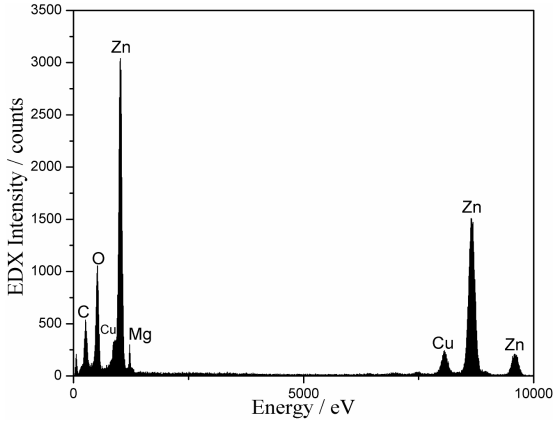

Fig. 4. EDX spectrum of the single nanowire.

Mg, C, Cu and O peaks are observed (the Cu peak comes from the TEM sample grid and the C peak comes mainly from atmospheric contamination due to the exposure of the sample to air [31]), confirming that the compositions of the products are Mg-doped ZnO without impurity. Similar results were obtained from different areas of the nanowires for several times.

3.4. Optical properties

Figure 5 shows the room temperature PL spectrum with He–Cd laser excitation at 325 nm. Both the Mg--doped and undoped samples show two emission bands: a narrow UV emission and a broad green emission. The UV emission is commonly originated from the free--exitonic recombination through an exciton–exciton collision process corresponding to the near band-edge emission of band gap ZnO [3]. Compared with the undoped one, the UV peak of the doped sample shifts to 378 nm from 383 nm. The peak at 378 nm and 383 nm corresponding to E_v = 3.28 eV and 3.24 eV, respectively, indicating that the band-gap energy has increased by the doping of Mg in the nanowire, because MgO (7.7 eV) has a wider band-gap than ZnO (3.37 eV) [32], in agreement with the XRD and EDX results. It is worthy to note that this blueshift is not associated by quantum confinement effects, because the average diameter of the nanowires is about 60 nm, far larger than the exciton Bohr radius ($\approx$ 1.8–2.0 nm) [33] of ZnO. The green emission is generally considered to be related to various intrinsic defects produced during ZnO preparation, but the exact mechanism is still unclear [34]. The presence of oxygen vacancies (V_O), zinc vacancies (V_{Zn}), interstitial zinc (Zn_i) and antisite defects (O_{Zn}) have been attributed to correspond to the green emission of ZnO by different researchers [35–37]. In our experiment, an interesting phenomenon is that the green band in the Mg-doped ZnO is much stronger than that of undoped ZnO. This may be attributed to surface-recombination effect on the thin--nanowires system [38]. Of course, the detailed explanation of PL will be given elsewhere.

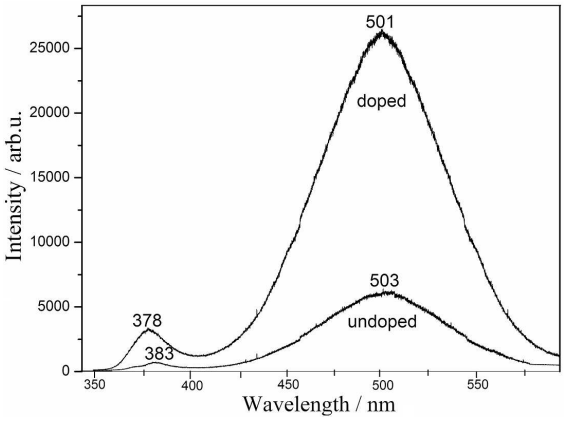

Fig. 5. Room temperature PL spetcrum of undoped and Mg-doped ZnO samples.

3.5. Growth mechanism

Vapor–liquid–solid (VLS) and vapor-solid (VS) mechanisms have been proposed to explain the formation of ZnO nanostructures. The VLS process begins from the absorption of the source materials from the gas phase into the metal liquid droplets and forms the liquid alloy. When this liquid alloy becomes saturated, a solid precipitate is formed which serves as a preferred site for further deposition. The dominant characteristic of the VLS mechanism is that a metal particle is located at the growth front of the nanowires and acts as the catalytic active sites. But in our work, even a thin layer of gold (12 nm) was coated on Si (111) substrate, but after the deposition no metal catalyst or any type of impurity was detected from the tips of the grown ZnO nanowires, as confirmed by the SEM and TEM observations. Therefore, we suggest that the growth mechanism of the product can be understood on the basis of the VS growth mechanism and small Au particles do not serve as catalysts in our case, but they simply offer favorable nucleation sites for nanowires growth. The Au thin film on Si substrates was expected to form nanosized Au–Si alloy droplets as the eutectic point of Au–Si binary system is about 363 ℃ [39] on the basis of their phase diagram. After the temperature rised above 800 ℃, active carbon and ZnO in the source materials begin to react with each other and produce Zn and/or ZnO_x vapor and then the Zn and/or ZnO_x and Mg vapors were transferred to the low temperature area and absorbed onto the Au–Si alloy droplets. Then solid ZnO will precipitate from droplet in the form of nanowires when ZnO reach the supersaturating state. Meanwhile, Mg was doped into the ZnO particles through the process of Mg substituting of Zn atom in ZnO. Continuous feeding of the reactants sustains the thickness of ZnO over the gold particles and gold lies beneath at the base of the formed ZnO nanowires [40]. Therefore, no sign of Au particles was observed from the tips of as-grown nanowires.

4. Conclusion

In summary, high-quality ZnO nanowires doped with Mg have been synthesized on Au-coated Si (111) substrates using CVD method at 850 ℃. According to the results of EDX analysis, the compositions of the products are Mg-doped ZnO without impurity, and Mg doping has not change the wurtzite structure of ZnO because of its small content. Most of the nanowires have diameters ranging from 50 to 80 nm and lengths up to hundreds of micrometres. Detailed structural characterizations indicate that the synthesized nanowires are single-crystalline and grow along the [0001] direction in preference, indicating that introduction of divalent Mg ion in the ZnO lattice did not affect the growth direction. The growth mechanism of ZnO nanowires can be explained by a VS growth model, and the as-deposited Au particles act as nucleation sites.

Acknowledgments

The authors are grateful for the financial support of the Key Research Program of the National Natural Science Foundation of China (No. 90301002 and No. 90201025).

References

[1] B. Tian, X. Zheng, T.J. Kempa, Y. Fang, N. Yu, G. Yu, J. Huang, C.M. Lieber, *Nature* **449**, 885 (2007).

[2] J.B. Shen, H.Z. Zhuang, D.X. Wang, C.S. Xue, H. Liu, *Cryst. Growth Des.* **9**, 2187 (2009).

[3] L. Feng, A. Liu, Y. Ma, M. Liu, B. Man, *Acta Phys. Pol. A* **117**, 257 (2010).

[4] W. Zaleszczyk, K. Fronc, E. Przezdziecka, E. Janik, A. Presz, M. Czapkiewicz, J. Wrobel, W. Paszkowicz, L. Klopotowski, G. Karczewski, T. Wojtowicz, *Acta Phys. Pol. A* **114**, 1451 (2008).

[5] W. Lee, M.C. Jeong, J.M. Myoung, *Appl. Phys. Lett.* **85**, 6167 (2004).

[6] S.W. Jung, W.I. Park, G.C. Yi, M. Kim, *Adv. Mater.* **15**, 1358 (2003).

[7] Y.L. Seu, L. Pang, Y.L. Chia, Y.T. Tseung, J.H. Chorng, *J. Phys. D, Appl. Phys.* **37**, 2274 (2004).

[8] J.S. Jie, G.Z. Wang, X.H. Han, Q.X. Yu, Y. Liao, G.P. Li, J.G. Hou, *Chem. Phys. Lett.* **387**, 466 (2004).

[9] M. Yan, H.T. Zhang, E.J. Widjaja, R.P.H. Chang, *J. Appl. Phys.* **94**, 5240 (2003).

[10] H.S. Chen, J.J. Qi, Y.H. Huang, Q.L. Liao, Y. Zhang, *Acta Phys. Chim. Sin.* **23**, 55 (2007).

[11] K. Gas, K. Fronc, P. Dziawa, W. Knoff, T. Wojciechowski, W. Zaleszczyk, A. Baranowska-Korczyc, J.F. Morhange, W. Paszkowicz, D. Elbaum, G. Karczewski, T. Wojtowicz, W. Szuszkiewicz, *Acta Phys. Pol. A* **116**, 868 (2009).

[12] G. Wang, Z.Z. Ye, H.P. He, H.P. Tang, J.S. Li, *J. Phys. D, Appl. Phys.* **40**, 5287 (2007).

[13] B.K. Sonawane, M.P. Bhole, D.S. Patil, *Opt. Quant. Electron.* **41**, 17 (2009).

[14] A. Rahm, T. Nobis, M. Lorenz, G. Zimmermann, N. Boukos, A. Travlos, M. Grundmann, *Adv. Solid State Phys.* **46**, 113 (2008).

[15] M. Lorenz, E.M. Kaidashev, A. Rahm, T. Nobis, J. Lenzner, G. Wagner, D. Spemann, H. Hochmuth, M. Grundmann, *Appl. Phys. Lett.* **86**, 143113 (2005).

[16] C. Czekalla, J. Guinard, C. Hanisch, B.Q. Cao, E.M. Kaidashev, N. Boukos, A. Travlos, J. Renard, B. Gayral, D.L. Dang, M. Lorenz, M. Grundmann, *Nanotechnology* **19**, 115202 (2008).

[17] R. Kling, C. Kirchner, T. Gruber, F. Reuss, A. Waag, *Nanotechnology* **15**, 1043 (2004).

[18] A.L. Yang, H.Y. Wei, X.L. Liu, H.P. Song, G.L. Zheng, Y. Guo, C.M. Jiao, S.Y. Yang, Q.S. Zhu, Z.G. Wang, *J. Cryst. Growth* **311**, 278 (2009).

[19] Y.Z. Zhang, J.G. Lu, Z.Z. Ye, Y.J. Zeng, L.P. Zhu, J.Y. Huang, *J. Phys. D, Appl. Phys.* **40**, 3490 (2007).

[20] H.C. Hsu, C.Y. Wu, H.M. Cheng, W.F. Hsieh, *Appl. Phys. Lett.* **89**, 013101 (2006).

[21] M. Zhi, L.P. Zhu, Z.Z. Ye, F. Wang, B. Zhao, *J. Phys. Chem. B* **109**, 23930 (2005).

[22] H. Pan, Y. Zhu, H. Sun, Y. Feng, C. Sow, J. Lin, *Nanotechnology* **17**, 5096 (2006).

[23] H.P. Tang, H.P. He, L.P. Zhu, Z.Z. Ye, M. Zhi, F. Yang, B. Zhao, *J. Phys. D, Appl. Phys.* **39**, 3764 (2006).

[24] C.J. Pan, H.C. Hsu, H.M. Cheng, C.Y. Wu, W.F. Hsieh, *J. Solid State Chem.* **180**, 1188 (2007).

[25] Q. Wei, M.K. Li, Z. Yang, L. Cao, W. Zang, H.W. Liang, *Acta Phys. Chim. Sin.* **24**, 793 (2008).

[26] X.C. Wu, J.M. Hong, Z.J. Han, Y.R. Tao, *Chem. Phys. Lett.* **373**, 28 (2003).

[27] J.S. Lee, Y.K. Byeun, S.H. Lee, S.C. Choi, *J. Alloys Comp.* **456**, 257 (2008).

[28] Y.C. Lin, W.T. Lin, *Nanotechnology* **16**, 1648 (2005).

[29] F. Wang, G.Q. Jin, X.Y. Guo, *J. Phys. Chem. B* **110**, 14546 (2006).

[30] R. Yousefi, B. Kamaluddin, *Appl Surf. Sci.* **256**, 329 (2009).

[31] J. Wang, H.Z. Zhuang, J.L. Li, P. Xu, *Acta Phys. Chim. Sin.* **26**, 2840 (2010).

[32] D. Qiu, H. Wu, N. Chen, *Chin. Phys. Lett.* **20**, 582 (2003).

[33] M. Yin, Y. Gu, I.L. Kuskovsky, T. Andelman, Y. Zhu, G.F. Neumark, S. O'Brien, *J. Am. Chem. Soc.* **126**, 6206 (2004).

[34] Y. Zhang, X. Song, J. Zheng, H. Liu, X. Li, L. You, *Nanotechnology* **17**, 1916 (2006).

[35] K. Vanheusden, C.H. Seager, W.L. Warren, D.R. Tallant, J.A. Voigt, *Appl. Phys. Lett.* **68**, 403 (1996).

[36] Y.W. Heo, D.P. Norton, S.J. Pearton, *J. Appl. Phys.* **98**, 073502 (2005).

[37] B. Lin, Z. Fu, Y. Jia, *Appl. Phys. Lett.* **79**, 943 (2001).

[38] I. Shalish, H. Temkin, V. Narayanamurti, *Phys. Rev. B* **69**, 245401 (2004).

[39] C.Y. Lee, T.Y. Tseng, S.Y. Li, P. Lin, *Tamkang J. Sci. Eng.* **6**, 127 (2003).

[40] D. Zhao, C. Andreazza, P. Andreazza, J. Ma, Y. Liu, D. Shen, *Chem. Phys. Lett.* **399**, 522 (2004).